Thiazolidinones: Potential human novel coronavirus (SARS-CoV-2) Protease Inhibitors against COVID-19

Vijay Kumar Vishvakarma[1,2], Indra Bahadur,[3,*] Ramesh Chandra,[2] Kamlesh Kumari,[4,*] Prashant Singh[1,*]

[1]Department of Chemistry, Atma Ram Sanatan Dharma College, University of Delhi, New Delhi, India; [2]Department of Chemistry, University of Delhi, Delhi, India; [3]Department of Chemistry, Faculty of Natural and Agricultural Sciences, North-West University, South Africa; [4]Department of Zoology, Deen Dayal Upadhyaya College, University of Delhi, New Delhi, India

*Corresponding author Email: biotechnano@gmail.com; psingh@arsd.du.ac.in and bahadur.indra@gmail.com

Abstract:

COVID-19 is a rapidly spreading infectious disease caused by a novel beta coronavirus SARS-CoV-2. During the 1980's coronavirus, genomic RNA was transcribed into a set of subgenomic mRNAs that encode viral proteins containing a leader sequence derived from the 5' end of the genome. The subgenomic mRNAs are transcribed from negative-strand RNAs, synthesized for the full-length genomic RNA - a unique mechanism, presumed to occur by a process involving viral polymerase jumping from one part of the genome template to another, leading to high rate of recombination for coronaviruses, playing role in viral interspecies infections. The sequence of SARS-CoV-2 confined that spike protein has furin cleavage site in the S1/S2 junction different from SARS-CoV and other closely related viruses. This has proved the possibility of Protease inhibitors as antivirals has led to the speculation about virulence and pathogenesis, and it is also possible that this new furin site may serve as a marker to identify a possible precursor virus. This novel human coronavirus (SARS-CoV-2) has resulted in a large number of fatalities and incapacitated human health system. No treatment is available, and a vaccine will not be available for several months. Hence, the protease of coronavirus is a promising target for antiviral drug discovery.

We herein report a new generation of thiazolidinone derivatives, inhibitors of SARS-CoV-2 coronavirus protease that incorporated thiazolidinone heterocycles as N-terminal capping groups of the peptide moiety. The compounds were extensively characterized with respect to inhibition of various proteases, inhibition mechanism, membrane permeability, antiviral activity. Our research group has recently designed a one-pot three-component reaction and its mechanism was studied through DFT. Further, a library of the molecules based on the products is designed. These novel molecules were screened through ADMET and molecular docking to find out the potential inhibitor of SARS-CoV-2 protease, as they may have competitive inhibition mechanisms, in correlation with their membrane permeability, a more pronounced antiviral activity.

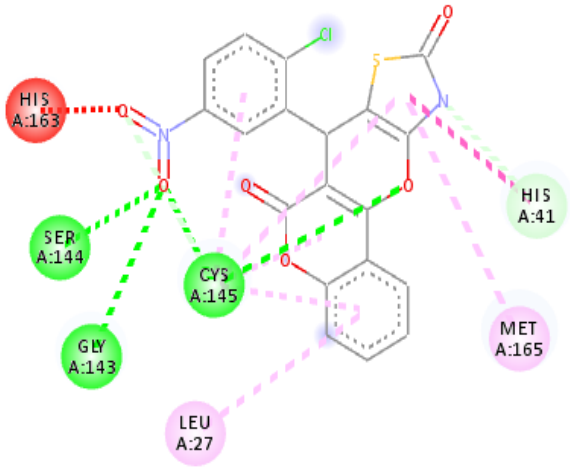

Keywords: SARS-CoV-2 protease; COVID-19; protease inhibitors; Docking; ADMET; antiviral activity.

1 Introduction

Several virus replications inhibiting drugs were discovered during the 1950s. However, the development of the new antiviral agents with activity against the virus-specific functions grew rapidly in recent years and several different antiviral chemotherapeutic agents have been approved for the treatment of individuals infected with a variety of different viruses including respiratory syncytial virus. The virus contains nucleic acid genomes which undergo replication as part of the virus life cycle. Therefore, the majority of the approved antiviral agents are nucleoside analogues, and act by inhibiting viral DNA synthesis or viral reverse transcription. The coronavirus is the world's only superpower today. December 2019 was a tragic day for the world when a new coronavirus caused an outbreak of pulmonary disease in the city of Wuhan in China. This COVID-19 pandemic caused by SARS-CoV-2 is now a global health emergency and is the greatest challenge, the world has faced since the second world war since more than 150 countries are already gravely affected. On the turn of the 21st century, researchers confronted to study coronaviruses - a family of enveloped positive-stranded RNA viruses with the question of coronavirus novelty with the severe acute respiratory syndrome (SARS) as is the case with the current outbreak of SARS-CoV-2, the causative agent of COVID-19. SARS-CoV-2 main proteinase controls the activities of the corona replication complex is an attractive target for therapy. Coronaviruses (CoVs) have a single-stranded RNA genome (26.2-31.7kb) spherical and characterized by bears club-shaped projections of glycoproteins on its surface. The structural proteins of CoV are spike (S) trimeric protein, membrane(M) protein, envelope (E) protein and the beta-CoVs also have hemagglutinin esterase (HE) glycoprotein. The best-characterized drug targets among coronaviruses are the main protease, an enzyme essential for processing the polyproteins that translated from viral RNA, chopping up the chain into functional proteins that the virus then uses to assemble itself and multiply. If we disrupt this key piece of the virus's self-replication machinery could bring an infection screeching to a halt. Hence inhibiting the activity of this enzyme would block viral replication, and in the absence of human proteases with cleavage specificity, inhibitors are unlikely to be toxic.[1-3] Most of the experimental laboratories are shut down due to novel coronavirus, SARS-CoV-2 spreading across the globe, stalled the efforts to monitor the virus. However, some labs are looking for druggable targets to treat COVID-19, a viral infection in the absence of any specific vaccine or drugs. Thus protease of SARS-CoV-2 is a promising target for antiviral drug discovery. [4-7] The imidazothiazole derivatives have pharmacological properties, such as anti-infectious, antiviral and others. Our research group is involved in the synthesis of heterocyclic compounds and evaluation of their

potential antiviral properties and other biological properties. One-pot multicomponent reactions are important in the present circumstances to synthesize thiazolidinones known for their antibacterial, antifungal, anticancer and antiviral activities by inhibiting the enzyme activities. Therefore, thiazolidinones have been prepared by one-pot multi-component reaction as inhibitors of SARS CoV-2 protease, may be a potential drug for treating COVID-19.[8-14]

Our in-silico approach provides a strategically efficient route to achieve as a potential candidate and insight for inhibiting the protease activity and to control the infection caused by SARS-CoV-2, as a fast and efficient approach. [4-6] Therefore, we have proposed a one-pot multicomponent reaction via aromatic aldehydes, chromane-2,4-dione and thiazolidine-2,4-dione to get the potential molecule as a protease inhibitor. The reaction mechanism of the synthesis has been studied by DFT. Further, a library of the compounds was designed to study their impact on the protease activity of SARS-CoV-2 via docking or molecular modeling.

Result

The docking of all the 100 designed compounds was performed against the protease of SARS-COV-2 and the data is available in **Table 3**. Compound number 34, 42, 55, 58, 60 and 93 showed the best binding with the protease of SARS-COV-2. The details of the energy contribution due to hydrogen bonding, electrostatic and van der Waal of the top six compounds is given in **Table 4**. Further, the drugs used in clinical trials are docked against the protease of SARS-COV-2 and the binding energy was determined, given in **Table 4a**. The docked posed of the top six compounds 34, 42, 55, 58, 60 and 93 showed the best binding with the protease of SARS-COV-2 are given in **Figure 2**. A details study of the interaction of the compounds number s34, 42, 55, 58, 60 and 93 against the protease of SARS-COV-2 is given in Table 5. Herein, the interaction (hydrogen bonds and hydrophobic) of the compounds with different amino-acids of the protease of SARS-CoV-2 with their distance is determined. Further, the top six compounds were analyzed by plotting the interacted amino-acids of the protease on interaction with the energy as in **Figure 3**.

ADMET Result

Physiochemical properties act as descriptors to describe the properties of drug.[15] For drug likeness and absorption, distribution, metabolism, excretion and toxicity (ADMET) properties, these descriptors play key role.

Physicochemical properties of the top six hits

Aqueous solubility of drug is highly important to describe the absorption and distribution properties. Poor solubility of drug mainly aims to bad absorption and leads to the failure of drug.[16] Herein, log S values of the drugs were calculated based on the structural features. Partition coefficient is defined as a ratio of concentrations of unionized compound among the two solvents. If one solvent is polar like water and other is non-polar like octanol then it is termed as lipophilicity or hydrophobicity.[16] Distribution coefficient (log $D_{7.4}$) is another form of log P. The basic differences between log P and log D is that log D is pH specific and also consider the ionic parts of drug while log P mainly consider neutral part.[17] The values of Log S, Log D7.4 and Log P are given in **Table 6**.

Absorption properties of the top six thiazolidinones

Based on the physicochemical descriptors, absorption properties in term of Caco-2 permeability, permeability glycoprotein (P-gp) for inhibitor and substrate, human intestinal absorption and bioavailability (F20% & F30%) were studied and given in **Table 7.** Caco-2 cells are part of colon carcinoma and have resemblance with epithelium of intestine. Caco-2 permeability measures the rate of reflux of drug to cross the Caco-2 monolayer.[18] The numerical value of Caco-2 permeability must be higher than -5.15 for the optimum permeability. The result the all the compounds have good permeability. Glycoprotein permeability indicates the efflux and mediated by P-gp. P-gp efflux indicates the efflux from liver, kidney, gastrointestinal tract and brain endothelium.[19] All the compounds have acceptable values.

Distribution properties of top six thiazolidinones

Distributional properties of top six thiazolidinones were calculated based on physicochemical descriptors. The distribution properties like plasma protein binding (PPB), volume distribution (VD) and blood brain barrier penetration (BBB) is given in **Table 8**.

When a drug reaches in blood it bind with plasma protein. The binding affinity of the compounds towards plasma proteins lowers its distribution through the cell membrane. Minimum the binding energy more efficient a drug will be.[20] All the compounds have acceptable PPB. Volume distribution is that volume of drug, which is necessary for a drug to maintain the sufficient concentration in the bloodstream. VD is responsible for the distribution of drug between plasma and rest of the body. More the value of VD, more will be the distribution of drug into the body tissue.[21] The values of VD < 0.07 L/kg correspond to

bind with plasma protein or highly hydrophilic, value of VD 0.07-0.7 L/kg corresponds to evenly distributed and VD > 0.7 L/kg corresponds to distribution towards tissue components (highly lipophilic). VD value indicates that all top-six compounds have high affinity towards the plasma protein. Central nervous system (CNS) mainly controls the whole body activity and blood-brain barrier (BBB) separate circulating blood of CNS from extracellular fluid of all rest body part. Drugs can be categorized by targeting and non-targeting CNS. When researchers developing non CNS targeting drug, it must be ensure that drug should not cross the blood brain barrier. BBB crossing drug can cause more risk of side effect.[22] BB ratio > 0.1 is BBB+ and BB ratio <0.1 is BBB-. The features selected for BBB permeation is H-bonds < 8-10, MW < 400-500 and no acids.

Metabolism properties of top six thiazolidinones

Metabolism is break down of a compound within the body after entering in the body. Metabolism of the drug/molecule is done in the liver by the redox enzymes. The most common types of redox enzyme is cytochrome P450.[23, 24] These metabolites are two types, pharmacologically active and inactive/ innert. In case of pharmacologically inert drug metabolism deactivates the amount of drug and resulted in the less effect by drug on the body. In case of active metabolite, metabolism enhances the activity of drug more than the drug. Metabolic properties for top-six compounds were calculated for different isozymes of cytochrome P450 in term of inhibitor and substrate. The main isozymes are CYP1A2, CYP3A4, CYP2C9, CYP2C19 and CYP2D6 and of 57 isozymes. These isozymes metabolize about two-thirds drugs and these five isozymes mainly contribute to almost 80%. The values for top-six compounds in term of cytochromes substrate (sub) and inhibitors (inh) were analyzed as in **Table 9.** All the compounds showed acceptable metabolic properties.

Excretion properties of top six thiazolidinones

Drug may be eliminated in its original state or eliminated after some modification. Excretion of a drug is followed by several routs but through kidney and liver are considered best. Excretion through renal duct is most common for the unchanged drug or its metabolites. Only water soluble and polarized drugs are excreted with urine.[25, 26] Lipid soluble drugs can't be excreted by kidney. Hence, they require hepatic metabolism to break them into soluble components to eliminate with urine. Hepatic metabolized drug are mainly excreted by the faeces.[27] The excretion of drug is measure in two terms half-life ($t_{1/2}$) and clearance rate (CL) and value for top-six compounds are given in **Table 10**.

The half-life of drug is time for the amount of drug reduced to its half. Basically drug excretion follows the first order kinetics. Hence, a graph between log of concentration of compound and time gives the values of clearance rate as a slope of graph. Half-life of excretion greater than 8 hours is high, 3-8 hours is moderate and less than 3h is low. All top-six compounds have half-life less than 3h. Clearance rate of excretion having values more than 15 is high, 15-5 is moderate and less than 5 is low. All top-six compounds follow low clearance rate.

Toxicity properties of top six thiazolidinones

It is highly challenging to develop a new drug without considering it toxicity properties. Many drugs developed by researchers faced clinical trial unable to reach in market due to undesired toxicity or side effect.[28] Optimizing drug likeness properties is the key to develop the new lead out. Drug discovery mainly focused on the effective binding of drug into the active site of receptor. Potency of drug is a key factor in early stage while toxicity properties decide its effectiveness and success.[29] To develop a new drug, there must be a fine balance between toxicity, potency and pharmacokinetics of drug. Toxicity is the potency of drug to damage the body parts of an organism. Based on the adverse effect of drug on the various body parts it is divided into various forms like cytotoxicity, hepatotoxicity, etc.[29, 30] Herein, numerous toxicity of top-six compounds were determined like the human Ether-à-go-go-Related Gene (hERG) blockers, human hepatotoxicity (H-HT), ames mutagenicity, skin sensitization, half maximal lethal dose (LD50), drug induced liver injury (DILI) and maximum recommended daily dose (FDAMDD) and the value are given in **Table 11**.

Human Ether-à-go-go-Related Gene (hERG) mainly encoded for the $K_v11.1$ protein part of potassium ion channel (hERG channel). The activity of heart is mainly maintained by the electrical signal and this signal is mediated by hERG channel.[31] The highest values of hERG blocker is found for 93 while the lowest for 58/60. Liver provide a clearance pass to orally administered drugs and toxins. The hepatocyte membrane is in close contact with the drugs hence, a drug mainly infect the hepatocyte and can damage the liver. The highest human hepatotoxicity (H-HT) value is found for F1 while lowest is for 34. The Ames test is performed to check the carcinogenic nature of compounds because mutation is directly linked to the carcinogenicity.[32] The highest Ames mutagenicity values is found for A209 while lowest Ames mutagenicity value is found for 42. Most of the drugs act as skin sensitizer and produces irritation and sensitization. It is an immunological response to reduce the effect produced by drug.[33] The highest skin sensitization value is found for 60/55/58 while the

lowest value is found for 93. Median lethal dose (LD_{50}) is the dose of drug responsible for the killing of 50 % population of the treated animals within the given time.[34] The highest toxicity is found for 63. Drug induced liver injury (DILI) is the prime cause of failure of liver in the recent time. Most of the lipophilic drugs are metabolized by the liver and they cause some injury during this.[35] The highest value of DILI is found for F185 while lowest value is found for D46 & D20. The Food and Drug Administration (FDA) recommended maximum daily dose (FDAMDD) of the database of about 1200 drugs and suggested for the new lead drug to follow the QSAR model of FDAMDD.[36] The highest value of FDAMDD is found for 93. The maximum upper limit of drug beyond which no side effect is recorded with proper efficacy is known as maximum recommended therapeutic dose (MRTD).[37] The highest MRTD dose is found for 58/60.

Conclusion

Based on the previous results, different thiazolidinones are potential inhibitors against the ns2b-ns3 protease of DENV. In the present, novel thiazolidinones were designed using one pot three component reaction and the mechanism of synthesis was studied through DFT approach. Their potential was check against the protease of SARS-COV-2 as well the results were compared with the repurposing drugs being used in clinical trials against the infection of SARS-COV-2. **COMD60** showed the best binding with the protease of SARS-COV-2 and expected to be a potential antiviral agent. COMP60 also possess acceptable lipophilicity and solubility. Highest bioavailability is found to COMP60 and COMP58. Moderate distribution and metabolism property was found for COMP60. Lowest LD50 value is found for COMP60. It also has less drug induced liver injury. ADMET results corroborate the docking result towards the potency of COMP60.

Experimental details

Designing of molecules and molecular docking

Designing of molecules

Theoretically, design a one-pot three-component reaction using via by taking benzaldehyde, chromane-2,4-dione and thiazolidine-2,4-dione (TZD) to get 7-phenyl-7,10-dihydro-6H,9H-chromeno[3',4':5,6]pyrano[2,3-d]thiazole-6,9-dione as in **Scheme 1**.

Proposed mechanism for the synthesis of 7-phenyl-7,10-dihydro-6H,9H-chromeno[3',4':5,6]pyrano[2,3-d]thiazole-6,9-dione

Mechanism of synthesis of 7-phenyl-7,10-dihydro-6H,9H-chromeno[3',4':5,6]pyrano[2,3-d]thiazole-6,9-dione was studied by the Gaussian 9.0 as in **Scheme 2**. Thiazolidine-2,4-dione (**1)** reacts with benzaldehyde (**2**) to given **3** after elimination of a water molecule. Further, 4-hydroxy-2H-chromen-2-one (**4**) reacts with **3** and to give **5**. Further, hydroxyl group attacks on the keto group within the molecule and results in formation of **6**. Then, removal of water occurs in **5** to give **6**, the molecule of interest.

Study the mechanism of synthesis by DFT

Density functional theory (DFT) uses the quantum mechanical approach to solve the Schrodinger equation for the N body electron system. It reduces the wave function to achieve the soluble solution. By solving the electron density wave function equation of N electron system, various energy state of the system with physiochemical parameters can be determined. The optimization of product, reactants and intermediated were performed by applying B3LYP theory and taking 6–311G as a basis set in Gaussian 9.0.[38] The values of HOMO and LUMO were calculated by DFT and used to calculate the physicochemical descriptors.[39-43] The HOMO is filled with the electron and donate the electron. While LUMO is empty and accept electron. The energy gap between HOMO and LUMO is known as HOMO~LUMO gap. The optimized energies of the reactant, intermediate and product molecule are used to describe the proposed mechanism of reaction for the synthesis of novel thiazolidine. DFT approach is used to optimize the molecules. The optimized energy of TZD (**1)** is found to -719.4 A.U. while the energy of benzaldehyde was found to -345.48 A.U. The product of **1** & **2** is **3** having energy value -988.87 A.U. suggested the formation of a stable product. **3** reacts with **4** having energy -572.26 and form an intermediate **5** having energy -1560.93 A.U. **5** goes chelation by the attack of lone pair of OH to the carbonyl group and form the stable intermediate **6** with energy of -1560.93 A.U. **6** loses one water molecule to give 7-phenyl-7,10-dihydro-6H,9H-chromeno[3',4':5,6]pyrano[2,3-d]thiazole-6,9-dione with an energy of -1484.51 A.U. The increase in energy suggests the loss of water. A graphical depiction of the energies of the reactants, intermediates and product is given in the **Figure 1**. Details of the HOMO, LUMO, optimized geometry and various energies values of reactants, intermediate and product are given in **Table 1**.

Derivatives of thiazolidinones based on Scheme 1

The parent compound was used to create the 99 virtual derivatives to screen against the protease of SARS-COV-2. **Scheme 2** contains benzaldehyde as one of the reactant and therefore, its derivatives are used to create the library as in **Table 2**. The potency of the designed molecules will be compared with the repurposing drugs used in the clinical trials.

Preparation of PDB of SARS-COV-2 main protease

The preparation of protease of SARS-COV-2 (PDB: ID- 6LU7) was done using UCSF Chimera 1.11.2 in the dock prep module. The replacement of incomplete residues, removal of solvents, adding hydrogen and charges were assigned according to the AMBER.ff14SB force field. All the designed moelcules were optimized and used for docking against the protease of SARS-COV-2. [44]

Molecular Docking

Molecular docking uses the computational tool to identify the interaction between small molecules and a protein just like the lock and key model. It allows to studies the interaction at atomic level in the active binding cavity of protein.[43, 45-58] Choosing a suitable parameter to get the lead compound is very important.[59][59][57] iGEMDOCK has several parameters and drug screening mode is used.[60] In this, population size (n = 200), number of solutions for each compound (s = 3) and generations (g = 70) is considered. All the compounds were docked against protease of SARS-COV-2 and top six compounds were selected based on lowest energy.[39, 61, 62] The energy of binding of ligand to the protein is given by **Equation 1**.

$$E_{Binding} = H_{bond} + vdW + Elec \quad (\mathbf{1})$$

H_{bond} stands for hydrogen bonding energy, vdW stands for van der Waal energy and Elec stands for electro statistic energy.

Post-Docking analysis and modeling

The top molecules were chosen based on the total binding energy as per equation **1**. Post dock screening was performed by iGEMDOCK.[44] The modeling of best poses of molecules was taken by the Discovery Studio Visualizer V-2017.2 of BIOVIA.

ADMET properties

Physiochemical properties act as descriptors to describe the properties of drug. For drug likeness and absorption, distribution, metabolism, excretion and toxicity (ADMET) properties, these descriptors play key role. Basically, fraction of molecules like functional group defines the probable properties of the drug. Molecular weight (MW), heavy atoms, aromatic heavy atoms, fraction of carbon having sp^3 hybridization, no. of rotatable bonds, H-bond donors, H-bond acceptors, molar refractivity, topological surface area (TPSA) solubility (log S), distribution coefficient (log $D_{7.4}$) and partition coefficient (log P) were calculated using the web server from the webserver (http://admet.scbdd.com/calcpre/index/). Based on the physicochemical properties ADMET properties were calculated.[15, 21, 27, 63-65]

References

1. **Alfahan, A., et al., *In the era of corona virus: health care professionals' knowledge, attitudes, and practice of hand hygiene in Saudi primary care centers: a cross-sectional study.* J Community Hosp Intern Med Perspect, 2016. 6(4): p. 32151.**
2. **Al-Hameed, F.M., *Spontaneous intracranial hemorrhage in a patient with Middle East respiratory syndrome corona virus.* Saudi Med J, 2017. 38(2): p. 196-200.**
3. **Al-Hazmi, A., *Challenges presented by MERS corona virus, and SARS corona virus to global health.* Saudi J Biol Sci, 2016. 23(4): p. 507-11.**
4. **Sahu, S., et al., *In silico ADMET study, docking, synthesis and antimalarial evaluation of thiazole-1,3,5-triazine derivatives as Pf-DHFR inhibitor.* Pharmacological Reports, 2019. 71(5): p. 762-767.**
5. **El Aissouq, A., et al., *In Silico Design of Novel Tetra-Substituted Pyridinylimidazoles Derivatives as c-Jun N-Terminal Kinase-3 Inhibitors, Using 2D/3D-QSAR Studies, Molecular Docking and ADMET Prediction.* International Journal of Peptide Research and Therapeutics, 2019.**
6. **Vian, M., et al., *In silico model for mutagenicity (Ames test), taking into account metabolism.* Mutagenesis, 2019. 34(1): p. 41-48.**
7. **Onen-Bayram, F.E., et al., *3-Propionyl-thiazolidine-4-carboxylic acid ethyl esters: a family of antiproliferative thiazolidines.* Medchemcomm, 2015. 6(1): p. 90-93.**
8. **Kumar, P.P., et al., *One pot, three-component synthesis of novel 3, 4-dihydrophthalazin-2(1H)-yl-4-phenyl-4H-pyrans.* Tetrahedron Letters, 2014. 55(14): p. 2177-2182.**
9. **Patel, D.S., J.R. Avalani, and D.K. Raval, *One-pot solvent-free rapid and green synthesis of 3,4-dihydropyrano[c]chromenes using grindstone chemistry.* Journal of Saudi Chemical Society, 2016. 20: p. S401-S405.**
10. **Wang X. M., Y.H.L., Qaun Z. J., Wang X. C.,, *One-pot synthesis of benzoquinoline and coumarin derivatives using Meldrum's acid in three-component reactions.* Res. Chem. Intermed., 2013. 39(6): p. 2357–2367.**
11. **Yavari, I., et al., *A one-pot synthesis of bis(phenylimino)thiazolidines from ketene N,S-acetals and N,N ',-diphenyloxalimidoyl dichloride.* Molecular Diversity, 2018. 22(1): p. 11-19.**
12. **Yang, J.G., et al., *One-pot three-component synthesis of tetrahydrobenzo[b]pyrans catalyzed by cost-effective ionic liquid in aqueous medium.* Chinese Journal of Chemical Engineering, 2015. 23(8): p. 1416-1420.**
13. **Singh, P., et al., *Synthesis and electrochemical studies of charge-transfer complexes of thiazolidine-2,4-dione with sigma and pi acceptors.* Spectrochim Acta A Mol Biomol Spectrosc, 2010. 75(3): p. 983-91.**
14. **Kumar, A., et al., *Nano-sized copper as an efficient catalyst for one pot three component synthesis of thiazolidine-2, 4-dione derivatives.* Catal Comm 2008. 10: p. 17-22.**
15. **Ferreira, L.L.G. and A.D. Andricopulo, *ADMET modeling approaches in drug discovery.* Drug Discovery Today, 2019. 24(5): p. 1157-1165.**
16. **Babic, I., et al., *Influence of flavonoids' lipophilicity on platelet aggregation.* Acta Pharmaceutica, 2019. 69(4): p. 607-619.**
17. **Nanavati, C. and D.E. Mager, *Calculated Log D Is Inversely Correlated With Select Camptothecin Clearance and Efficacy in Colon Cancer Xenografts.* Journal of Pharmaceutical Sciences, 2016. 105(4): p. 1561-1566.**
18. **Rodriguez-Rosales, R.J. and Y. Yao, *Phytoglycogen, a natural dendrimer-like glucan, improves the soluble amount and Caco-2 monolayer permeation of curcumin and enhances its efficacy to reduce HeLa cell viability.* Food Hydrocolloids, 2020. 100.**
19. **Feldmann, M., et al., *P-glycoprotein (Pgp) overactivity in pharmacoresistant epilepsy patients with focal cortical dysplasia compared to healthy controls measured using (R)-***

[11C] verapamil PET and the Pgp inhibitor Tariquidar. **European Journal of Neurology, 2014. 21: p. 229-229.**

20. **Ma, C.Y., et al., *Prediction models of human plasma protein binding rate and oral bioavailability derived by using GA-CG-SVM method.* Journal of Pharmaceutical and Biomedical Analysis, 2008. 47(4-5): p. 677-682.**
21. **Wang, N.N., et al., *ADME Properties Evaluation in Drug Discovery: Prediction of Caco-2 Cell Permeability Using a Combination of NSGA-II and Boosting.* Journal of Chemical Information and Modeling, 2016. 56(4): p. 763-773.**
22. **Bao, X., et al., *Protein Expression and Functional Relevance of Efflux and Uptake Drug Transporters at the Blood-Brain Barrier of Human Brain and Glioblastoma.* Clinical Pharmacology & Therapeutics, 2019.**
23. **Rostkowski, M., O. Spjuth, and P. Rydberg, *WhichCyp: prediction of cytochromes P450 inhibition.* Bioinformatics, 2013. 29(16): p. 2051-2052.**
24. **Su, B.H., et al., *Rule-Based Prediction Models of Cytochrome P450 Inhibition.* Journal of Chemical Information and Modeling, 2015. 55(7): p. 1426-1434.**
25. **Daina, A., O. Michielin, and V. Zoete, *SwissADME: a free web tool to evaluate pharmacokinetics, drug-likeness and medicinal chemistry friendliness of small molecules.* Sci Rep, 2017. 7: p. 42717.**
26. **Vishvakarma, V.K.S., P.; Kumar, V.; Kumari, K.; Patel, R.; Chandra, R.;, *Pyrrolothiazolones as Potential Inhibitors for the nsP2B-nsP3 Protease of Dengue Virus and Their Mechanism of Synthesis.* Chemistryselect, 2019. 4(32): p. 9410-9419.**
27. **Guan, L.F., et al., *ADMET-score - a comprehensive scoring function for evaluation of chemical drug-likeness.* Medchemcomm, 2019. 10(1): p. 148-157.**
28. **Celik, S., et al., *Synthesis, molecular docking and ADMET study of ionic liquid as anticancer inhibitors of DNA and COX-2, TOPII enzymes.* Journal of Biomolecular Structure & Dynamics, 2019. 7: p. 1-11.**
29. **Deo, K.M., et al., *Synthesis, characterisation and potent cytotoxicity of unconventional platinum(iv) complexes with modified lipophilicity.* Dalton Transactions, 2019. 48(46): p. 17217-17227.**
30. **Di, L. and E.H. Kerns, *Application of pharmaceutical profiling assays for optimization of drug-like properties.* Current Opinion in Drug Discovery & Development, 2005. 8(4): p. 495-504.**
31. **Hull, C.M., et al., *Investigating the utility of adult zebrafish ex vivo whole hearts to pharmacologically screen hERG channel activator compounds.* American Journal of Physiology-Regulatory Integrative and Comparative Physiology, 2019. 317(6): p. R921-R931.**
32. **Benfenati, E., et al., *A large comparison of integrated SAR/QSAR models of the Ames test for mutagenicity($).* Sar and Qsar in Environmental Research, 2018. 29(8): p. 591-611.**
33. **Wilm, A., et al., *Skin Doctor: Machine Learning Models for Skin Sensitization Prediction that Provide Estimates and Indicators of Prediction Reliability.* International Journal of Molecular Sciences, 2019. 20(19).**
34. **Alvarez-Holguin, A., et al., *Mean lethal dose (LD50) and growth reduction (GR(50)) due to gamma radiation in Wilman lovegrass (Eragrostis superba).* Revista Mexicana De Ciencias Pecuarias, 2019. 10(1): p. 227-238.**
35. **Mullins, C., K. Beaulac, and L. Sylvia, *Drug-Induced Liver Injury (DILI) With Micafungin: The Importance of Causality Assessment.* Annals of Pharmacotherapy, 2019.**
36. **Liu, T., et al., *Estimation of Maximum Recommended Therapeutic Dose Using Predicted Promiscuity and Potency.* Cts-Clinical and Translational Science, 2016. 9(6): p. 311-320.**
37. **Branham, M.L., E.A. Ross, and T. Govender, *Predictive Models for Maximum Recommended Therapeutic Dose of Antiretroviral Drugs.* Computational and Mathematical Methods in Medicine, 2012.**

38. **Frisch, M.J.T., G. W.; Schlegel, H. B.; Scuseria, G. E.; Robb, M. A.; Cheeseman, J. R.; Scalmani, G.; Barone, V.; Petersson, G. A.; Nakatsuji, H.; Li, X.; Caricato, M.; Marenich, A. V.; Bloino, J.; Janesko, B. G.; Gomperts, R.; Mennucci, B.; Hratchian, H. P.; Ortiz, J. V.; Izmaylov, A. F.; Sonnenberg, J. L.; Williams-Young, D.; Ding, F.; Lipparini, F.; Egidi, F.; Goings, J.; Peng, B.; Petrone, A.; Henderson, T.; Ranasinghe, D.; Zakrzewski, V. G.; Gao, J.; Rega, N.; Zheng, G.; Liang, W.; Hada, M.; Ehara, M.; Toyota, K.; Fukuda, R.; Hasegawa, J.; Ishida, M.; Nakajima, T.; Honda, Y.; Kitao, O.; Nakai, H.; Vreven, T.; Throssell, K.; Montgomery, J. A., Jr.; Peralta, J. E.; Ogliaro, F.; Bearpark, M. J.; Heyd, J. J.; Brothers, E. N.; Kudin, K. N.; Staroverov, V. N.; Keith, T. A.; Kobayashi, R.; Normand, J.; Raghavachari, K.; Rendell, A. P.; Burant, J. C.; Iyengar, S. S.; Tomasi, J.; Cossi, M.; Millam, J. M.; Klene, M.; Adamo, C.; Cammi, R.; Ochterski, J. W.; Martin, R. L.; Morokuma, K.; Farkas, O.; Foresman, J. B.; Fox, D. J., *Gaussian 16, Revision C.01.* 2016.**

39. **Vishvakarma, V.K., K. Kumari, and P. Singh, *A Model To Study The Inhibition Of Arginase II With Noscapine & Its Derivatives.* J Pro Res Bioinf 2020. 2(1): p. 1-14.**

40. **Kumar, D., et al., *Development of a theoretical model for the inhibition of nsP3 protease of Chikungunya virus using pyranooxazoles.* J Biomol Struct Dyn, 2020. 30(10): p. 3018-3034.**

41. **Vishvakarma, V.K., et al., *Pyrrolothiazolones as Potential Inhibitors for the nsP2B-nsP3 Protease of Dengue Virus and Their Mechanism of Synthesis* ChemistrySelect 2019. 4(32): p. 9410-9419.**

42. **Vishvakarma, V.K., et al., *A model to study the inhibition of nsP2B-nsP3 protease of dengue virus with imidazole, oxazole, triazole thiadiazole, and thiazolidine based scaffolds.* Heliyon, 2019. 5(8): p. e02124.**

43. **Singh, P., et al., *Computational approach to study the synthesis of noscapine and potential of stereoisomers against nsP3 protease of CHIKV.* Heliyon, 2019. 5(12): p. e02795.**

44. **Yang, J.M. and C.C. Chen, *GEMDOCK: A generic evolutionary method for molecular docking.* Proteins-Structure Function and Bioinformatics, 2004. 55(2): p. 288-304.**

45. **Kumar, D., et al., *Promising inhibitors of main protease of novel corona virus to prevent the spread of COVID-19 using docking and molecular dynamics simulation.* J Biomol Struct Dyn, 2020: p. 1-15.**

46. **Kumar, D., et al., *Selective Docking of Pyranooxazoles Against nsP2 of CHIKV Eluted Through Isothermally and Non-Isothermally MD simulations.* ChemistrySelect, 2020. 5(14): p. 4210-4220.**

47. **Kumar, D., et al., *Understanding the binding affinity of noscapines with protease of SARS-CoV-2 for COVID-19 using MD simulations at different temperatures.* J Biomol Struct Dyn, 2020: p. 1-14.**

48. **Kumar, D., et al., *A Theoretical Model to Study the Interaction of Erythro-Noscapines with nsP3 protease of Chikungunya Virus* ChemistrySelect 2019. 4(17): p. 4892-4900.**

49. **Vishvakarma, V.K., et al., *Rational Design of Threo as Well Erythro Noscapines, an Anticancer Drug: A Molecular Docking and Molecular Dynamic Approach* Biochemistry & Pharmacology 2017. 6(3): p. 1-7.**

50. **Vishvakarma, V.K., et al., *Interaction between Bovine Serum Albumin and Gemini Surfactants using Molecular Docking Characterization* Inf Sci Lett, 2017. 3: p. 1-9.**

51. **Singh, P., et al., *Computational docking studies of Noscapines: A potential bioactive agent* Amer J Pharmacol Pharmacother, 2017. 4(1): p. 9-14.**

52. **Kumar, D., et al., *Impact of Gemini Surfactants on the stability of Insulin using computational tools* J Nanomed Biother 2017. 7: p. 1-5.**

53. **Singh, P., K. Kumari, and R. Chandra, *Green synthesis of Tetrazines and their role as human cytomegalovirus (HCMV) protease inhibitor* J Theor Comp Sci 2016. 3: p. 1-5.**

54. **Singh, P., K. Kumari, and R. Chandra, *Synthesis, Computational & Docking Studies of Bis-(4-Hydroxycoumarin-3-Yl) Methanes As Potential Inhibitor For Carbonic Anhydrase, Glyceraldehyde-3-Phosphate Dehydrogenase* J Pharm App Chem 2016. 2: p. 81-101.**

55. **Singh, P., et al., *Virtual Screening and Docking Studies of Synthesized Chalcones: Potent Anti-Malarial Drug* Inter J Drug Dev Res 2016. 8(1): p. 49-56.**

56. **Patel, R., et al., *Interaction between pyrolidium based ionic liquid and bouvine serum albumin: A Spectroscopic and molecular docking insight* Biochem Anal Biochem 2016. 5: p. 1-8.**

57. **Chakravarty, A.K., P. Singh, and K. Kumari, *One pot green synthesis of biological potent thiazolopyrans and docking against human pancreatic lipase related protein 1 receptors* Inter J Curr Adv Res 2016. 5(1): p. 559-563.**

58. **Vishvakarma, V.K., et al., *Theoretical model to investigate the alkyl chain and anion dependent interactions of gemini surfactant with bovine serum albumin.* Spectrochim Acta A Mol Biomol Spectrosc, 2015. 143: p. 319-23.**

59. **Shareef, M.A., et al., *Design, synthesis, and antimicrobial evaluation of 1,4-dihydroindeno[1,2-c]pyrazole tethered carbohydrazide hybrids: exploring their in silico ADMET, ergosterol inhibition and ROS inducing potential.* Medchemcomm, 2019. 10(5): p. 806-813.**

60. **Hsu, K.C., et al., *iGEMDOCK: a graphical environment of enhancing GEMDOCK using pharmacological interactions and post-screening analysis.* Bmc Bioinformatics, 2011. 12.**

61. **Vijay, K.V., K. Kamlesh, and S. Prashant, *Inhibition of Protease of Novel Corona Virus by Designed Noscapines: Molecular Docking and ADMET Studies.* ChemRxiv, 2020.**

62. **Durgesh, K., K. Kamlesh, and S. Prashant, *A Theoretical Model to Study the Interaction Between Boronic Acids and Insulin.* ChemRxiv, 2020.**

63. **Tian, S., et al., *ADME Evaluation in Drug Discovery. 9. Prediction of Oral Bioavailability in Humans Based on Molecular Properties and Structural Fingerprints.* Molecular Pharmaceutics, 2011. 8(3): p. 841-851.**

64. **Wu, Z.X., et al., *ADMET Evaluation in Drug Discovery. 19. Reliable Prediction of Human Cytochrome P450 Inhibition Using Artificial Intelligence Approaches.* Journal of Chemical Information and Modeling, 2019. 59(11): p. 4587-4601.**

65. **Yang, H.B., et al., *admetSAR 2.0: web-service for prediction and optimization of chemical ADMET properties.* Bioinformatics, 2019. 35(6): p. 1067-1069.**

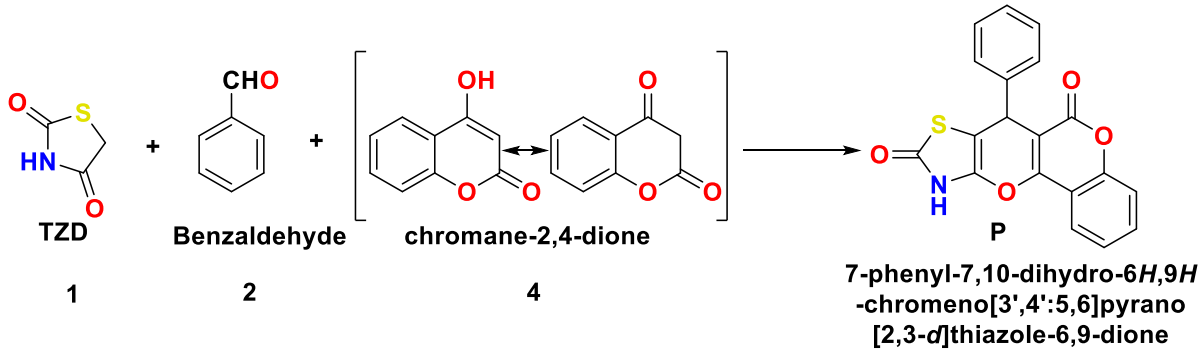

533

534 **Scheme 1** Synthesis of 7-phenyl-7,10-dihydro-6H,9H-chromeno[3',4':5,6]pyrano[2,3-

535 d]thiazole-6,9-dione

536

537

538

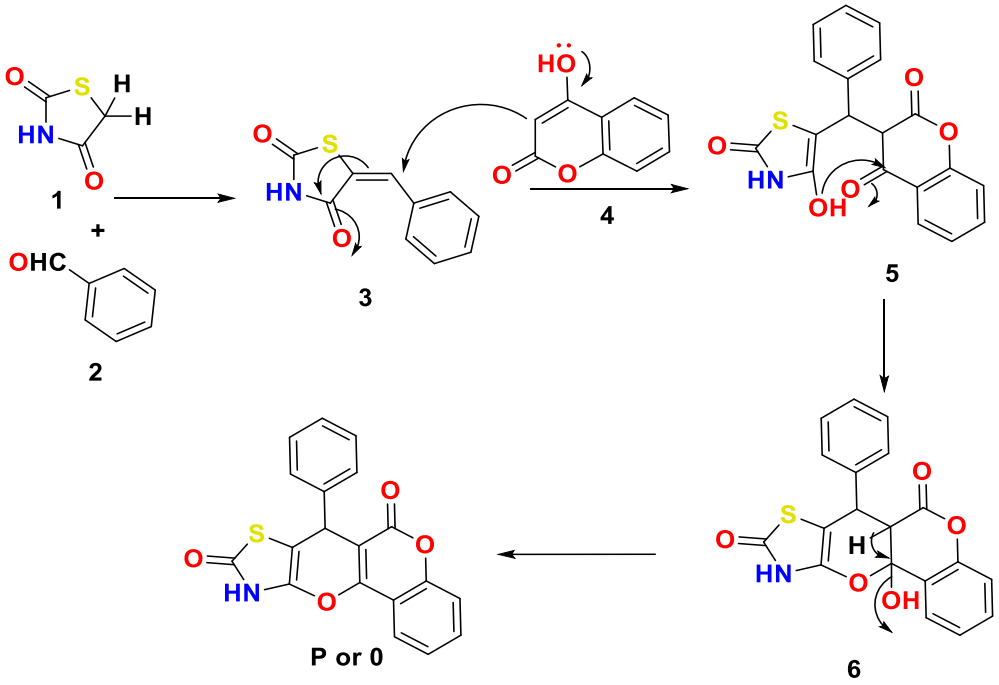

Scheme 2 Proposed mechanism of synthesis of 7-phenyl-7,10-dihydro-6H,9H-chromeno[3',4':5,6]pyrano[2,3-d]thiazole-6,9-dione i.e. thiazolidinones

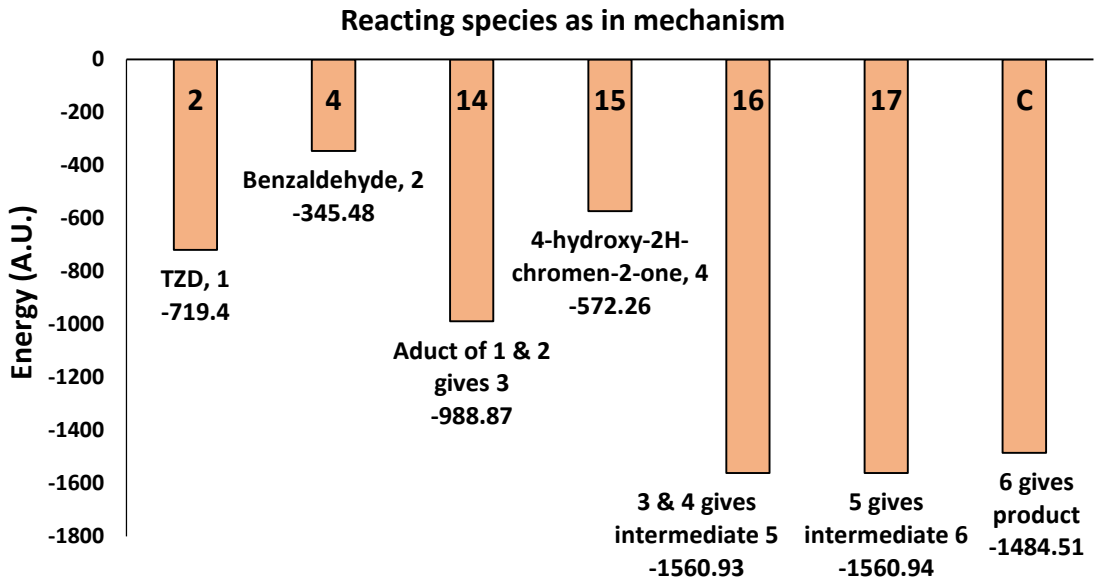

Figure 1 Analysis for the mechanism for the synthesis of 7-phenyl-7,10-dihydro-6H,9H-chromeno[3',4':5,6]pyrano[2,3-d]thiazole-6,9-dione as in **Scheme 2**

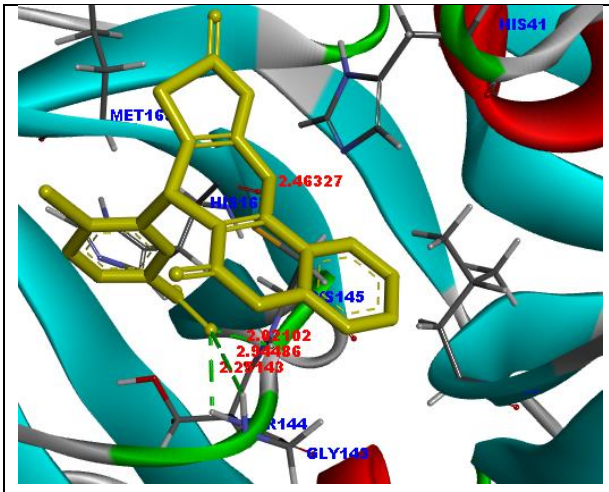	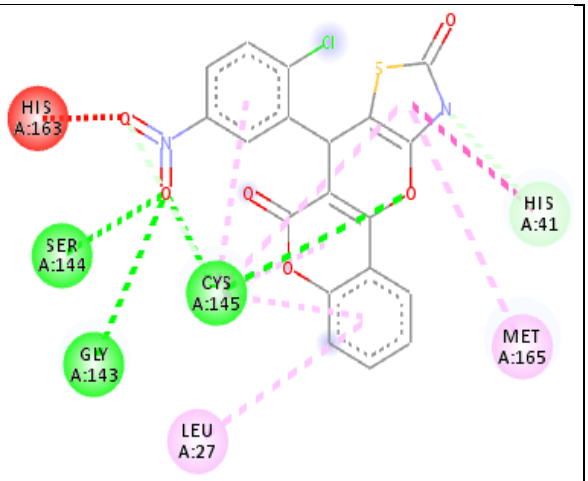
60	**60**
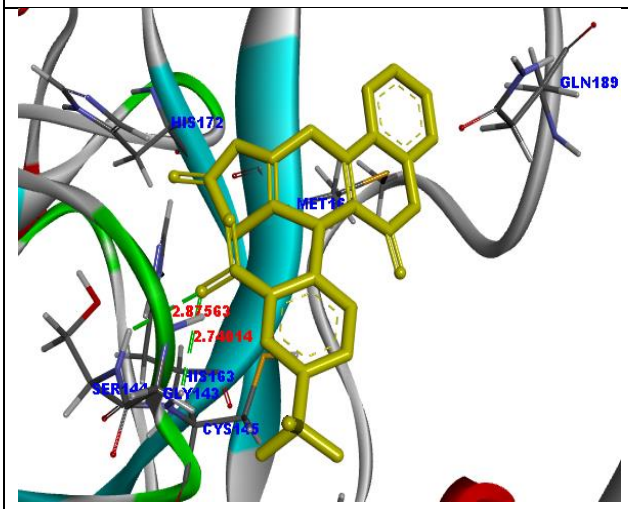	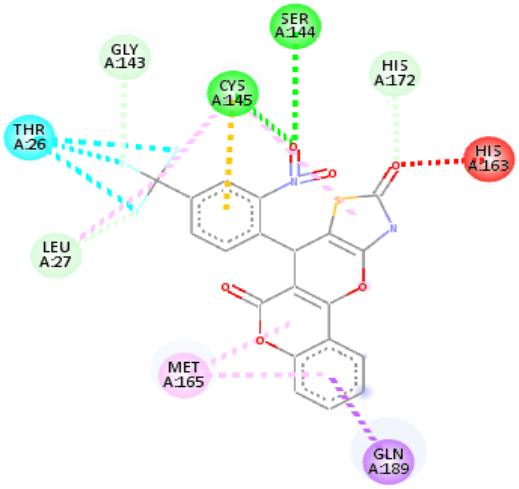
93	**93**
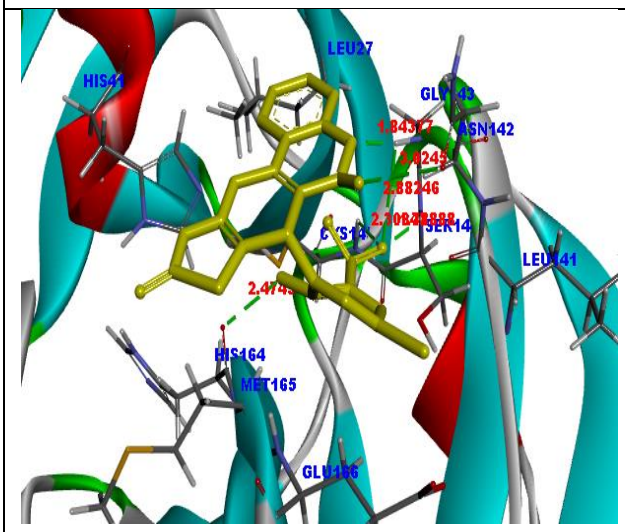	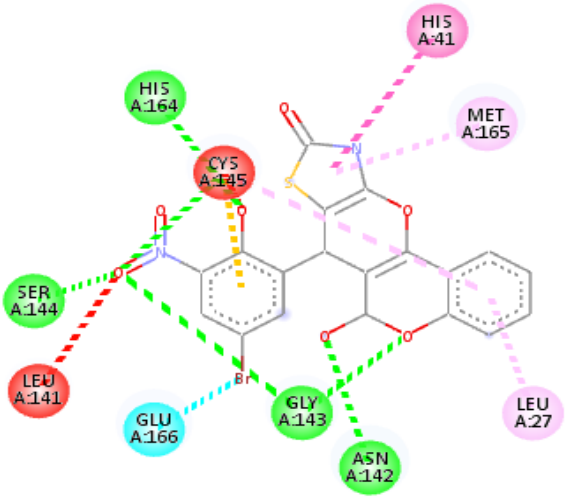
34	**34**

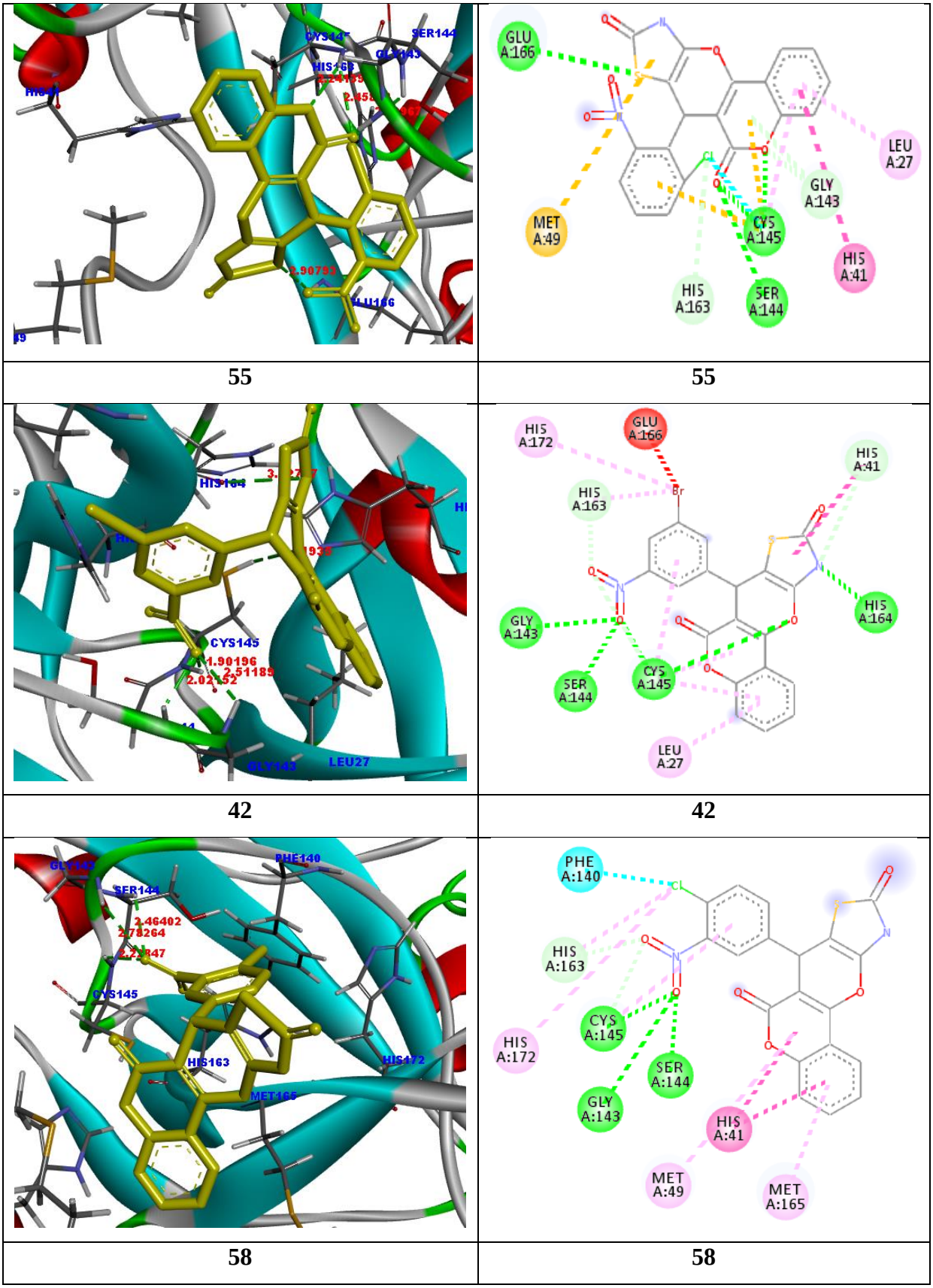

Figure 2 docked posed of compounds 34, 42, 55, 58, 60 and 93 with the protease of SARS-COV-2

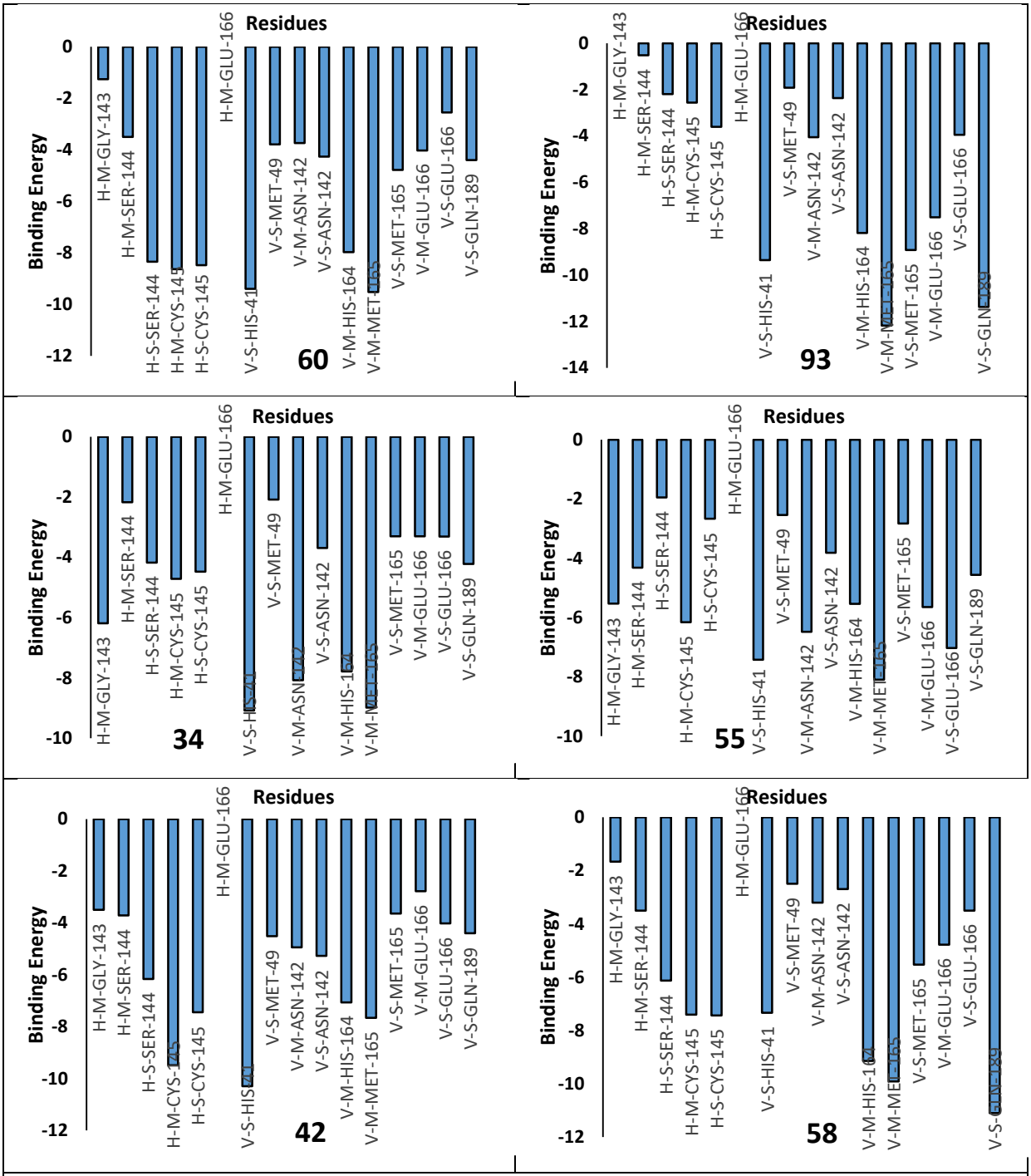

Figure 3 Energy contributed by amino-acids of the protease on interaction with the 60, 93, 34, 55, 42 and 58

551

552 **Table 1** HOMO, LUMO optimized geometry & energies values of the reactants,
553 intermediates and product as in **Scheme 2**

554

S. N.	HOMO	LUMO	Opt. geometry	Energies	
1	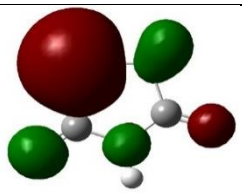	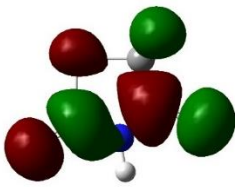	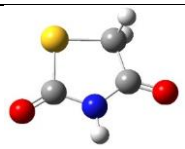	HOMO	-0.2770
				LUMO	-0.0583
				ΔE	0.2187
				E	-719.4
2	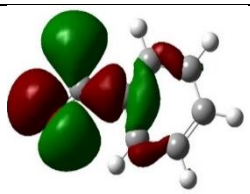	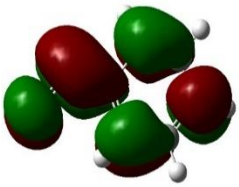	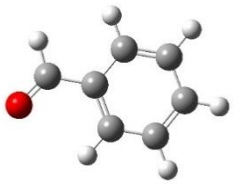	HOMO	-0.2569
				LUMO	-0.0699
				ΔE	0.1870
				E	-345.48
3	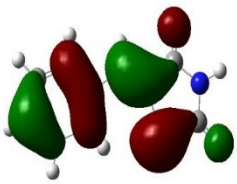	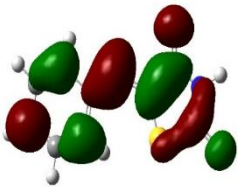	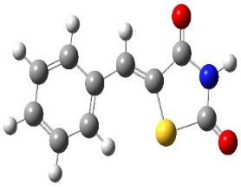	HOMO	-0.2398
				LUMO	-0.0924
				ΔE	0.1474
				E	-988.87
4	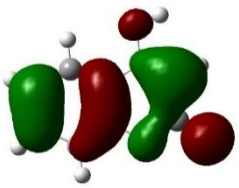	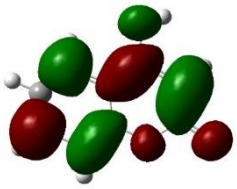	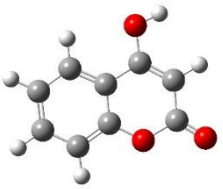	HOMO	-0.2352
				LUMO	-0.0587
				ΔE	0.1764
				E	-572.26
5	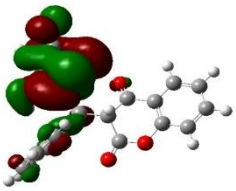	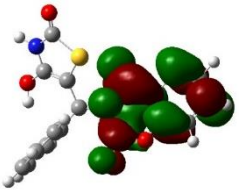	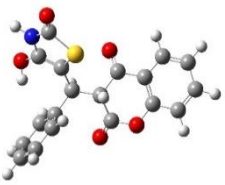	HOMO	-0.1987
				LUMO	-0.0806
				ΔE	0.1181
				E	-1560.9
6	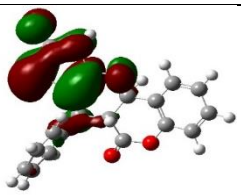	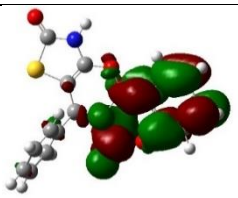	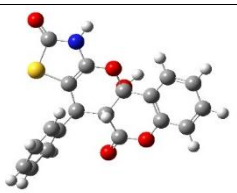	HOMO	-0.2059
				LUMO	-0.0418
				ΔE	0.1641
				E	-1560.9
P	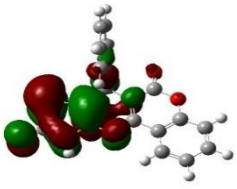	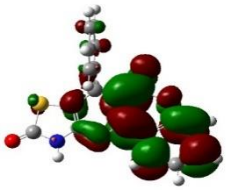	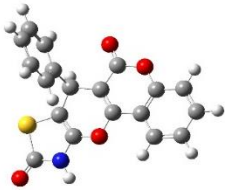	HOMO	-0.2174
				LUMO	-0.0740
				ΔE	0.1433
				E	-1484.5

555

556

Table 2 Designing the library of thiazolidinones on varying the aromatic aldehyde

S.N.	Substituent's positions on aryl part of aldehyde				
	2	**3**	**4**	**5**	**6**
0	-H	-H	-H	-H	-H
1	-H	-OMe	-O-CH_2-CH_2-Br	-H	-H
2	-H	-OMe	-OMe	-OMe	-Br
3	-Br	-H	-H	-OMe	-OH
4	-NH_2	-Br	-H	-Br	-H
5	-OMe	-Br	-H	-Br	-H
6	-OH	-Br	-H	-Br	-H
7	-H	-Br	-OH	-Br	-H
8	-H	-Cl	-OH	-Br	-H
9	-H	-Br	-OMe	-Br	-H
10	-H	-OMe	-OMe	-Br	-H
11	-H	-OMe	-OH	-Br	-H
12	-OH	-Br	-H	-Cl	-H
13	-OH	-Br	-H	-NO_2	-H
14	-H	-H	-OMe	-OH	-Br
15	-OH	-Br	-H	-H	-H
16	-OH	-O-C_2H_5	-H	-Br	-Br
17	-OMe	-H	-OMe	-Br	-H
18	-OMe	-H	-OH	-Br	-H
19	-Br	-H	-OMe	-OMe	-H
20	-Br	-H	-OMe	-OH	-H
21	-Br	-H	-H	-Br	-H
22	-H	-NO_2	-Br	-H	-H
23	-Br	-H	-H	-OMe	-H
24	-Br	-H	-H	-OH	-H
25	-Br	-H	-CH_3	-H	-H
26	-H	-H	-CH_3	-Br	-H
27	-H	-H	-OMe	-Br	-H
28	-H	-H	-OH	-Br	-H
29	-Br	-H	-Cl	-H	-H
30	-Br	-H	-OMe	-H	-H
31	-Br	-CHO	-H	-H	-H
32	-Br	-H	-H	-H	-H
33	-OMe	-OMe	-H	-Br	-H
34	-OH	-NO_2	-H	-Br	-H
35	-OH	-OMe	-H	-Br	-H
36	-NO_2	-H	-Br	-H	-H
37	-OMe	-H	-Br	-H	-H
38	-OH	-H	-Br	-H	-H
39	-H	-Br	-H	-H	-OH

40	-H	-Br	-H	-Br	-H
41	-H	-Cl	-H	-Cl	-H
42	-H	$-NO_2$	-H	-Br	-H
43	-H	-Br	-H	-H	-H
44	-H	-H	-Br	-H	-H
45	-H	-H	$-N(C_2H_4Cl)_2$	-H	-H
46	-Cl	-H	-OMe	-OMe	-Cl
47	-H	-OMe	-OMe	-Cl	-H
48	-H	-OMe	-OH	-Cl	-H
49	-OH	-Cl	-H	-Cl	-H
50	-H	-H	-OMe	-OMe	-Cl
51	-H	-H	-OMe	-OH	-Cl
52	-Cl	-H	-H	-H	$-CH_3$
53	-OH	-Cl	-H	-H	-H
54	-Cl	-H	-H	-H	-Cl
55	-Cl	-H	-H	-H	$-NO_2$
56	-Cl	-H	-H	-H	-OH
57	-H	-Cl	-Cl	-Cl	-H
58	-H	$-NO_2$	-Cl	-H	-H
59	-Cl	-H	-H	-Cl	-H
60	-Cl	-H	-H	$-NO_2$	-H
61	-Cl	-H	-H	-Cl	-Cl
62	-Cl	-H	-Me	-H	-H
63	-H	-H	-Me	-Cl	-H
64	-H	-H	-Cl	-Cl	-H
65	-H	-H	-OMe	-Cl	-H
66	-H	-H	-OH	-Cl	-H
67	-Cl	-H	-Cl	-H	-H
68	-Cl	-H	-OH	-H	-H
69	-Cl	-Cl	-H	-H	-H
70	-Cl	-OMe	-H	-H	-H
71	-Cl	-OH	-H	-H	-H
72	-Cl	-H	-H	-H	-H
73	-OMe	-OMe	-H	-Cl	-H
74	-OH	-OMe	-H	-Cl	-H
75	$-NO_2$	-H	-Cl	-H	-H
76	-OMe	-H	-Cl	-H	-H
77	-H	-Cl	-H	-H	NO_2
78	-H	-Cl	-H	-H	-OH
79	-H	-Cl	-H	-Cl	-H
80	-H	-Cl	-H	-H	-H
81	-H	-H	-Cl	-H	-H
82	-Cl	$-CF_3$	-H	-H	-H

83	-F	-CF_3	-H	-H	-H
84	-CF_3	-H	-H	-H	-F
85	-CF_3	-H	-H	-CF_3	-H
86	-CF_3	-H	-CF_3	-H	-H
87	-H	-H	-Cl	-CF_3	-H
88	-H	-H	-F	-CF_3	-H
89	-CF_3	-H	-F	-H	-H
90	-CF_3	-H	-H	-H	-H
91	-F	-Cl	-H	-CF_3	-H
92	-F	-H	-CF_3	-H	-H
93	-NO_2	-H	-CF_3	-H	-H
94	-H	-CF_3	-H	-H	-Cl
95	-H	-CF_3	-H	-H	-F
96	-H	-CF3	-H	-CF_3	-H
97	-H	-F	-H	-CF_3	-H
98	-H	-CF_3	-H	-H	-H
99	-H	-H	-CF_3	-H	-H
100	-O-CF_3	-H	-H	-H	-H

Table 3 Binding energy of the designed molecules i.e. thiazolidinones (0-99) against the protease of SARS-COV-2

C. No.	Total Energy	C. No.	Total Energy	C. No.	Total Energy	C. No.	Total Energy
0	-103.55	25	-104.031	50	-111.603	75	-123.204
1	-107.701	26	-106.624	51	-113.964	76	-113.278
2	-121.514	27	-106.881	52	-105.448	77	-115.895
3	-118.534	28	-107.273	53	-112.021	78	-107.294
4	-109.654	29	-110.676	54	-115.149	79	-109.432
5	-118.41	30	-110.686	55	-127.526	80	-105.223
6	-109.743	31	-119.633	56	-111.264	81	-105.202
7	-107.148	32	-99.8576	57	-107.673	82	-109.748
8	-106.913	33	-117.99	58	-124.746	83	-115.729
9	-108.296	34	-128.6	59	-102.491	84	-114.573
10	-109.287	35	-112.327	60	-135.77	85	-118.683
11	-105.056	36	-116.326	61	-104.549	86	-123.132
12	-110.761	37	-111.994	62	-106.168	87	-113.923
13	-117.551	38	-110.746	63	-108.138	88	-107.365
14	-111.07	39	-108.884	64	-106.497	89	-112.351
15	-110.399	40	-101.055	65	-107.46	90	-112.544
16	-113.723	41	-106.873	66	-105.802	91	-109.986
17	-106.56	42	-126.715	67	-97.7663	92	-109.529
18	-120.263	43	-106.497	68	-112.609	93	-129.464
19	-120.304	44	-105.14	69	-108.201	94	-100.907
20	-114.991	45	-110.747	70	-113.226	95	-109.487
21	-112.805	46	-111.338	71	-122.674	96	-111.982
22	-122.622	47	-104.723	72	-108.422	97	-112.753
23	-117.902	48	-110.12	73	-117.525	98	-113.016
24	-114.44	49	-100.534	74	-110.906	99	-109.837

564 **Table 4** Compounds number 34, 42, 55, 58, 60 and 93 showed the best binding with the
565 protease of SARS-COV-2

C. No.	Total Energy	E_{VDW}	E_{HBond}	E_{Elec}
60	-135.77	-92.5376	-44.2146	0.982384
93	-129.464	-117.664	-12.3849	0.58528
34	-128.6	-100.732	-28.8356	0.967276
55	-127.526	-104.378	-22.5981	-0.54959
42	-126.715	-86.5302	-40.9819	0.797261
58	-124.746	-90.5023	-35.1325	0.889179

566

567

568 **Table 4a** Binding energy of the repurposing drugs against the protease of SARS-COV-2 used
569 in clinical trials

Compound name	T. Energy	VDW	HBond	Elec
N3	-116.132	-104.716	-11.4159	0
Camostat	-114.554	-94.6993	-17.4391	-2.41559
Remdesivir	-105.955	-82.4292	-23.5262	0
Baricitinib	-94.5708	-62.9297	-31.641	0
Favipiravir	-93.8858	-57.7481	-36.1377	0
Galidesivir	-91.6304	-59.05	-32.5804	0
Darunavir-2	-91.3952	-73.1994	-18.1957	0
Thalidomide	-88.7425	-69.6454	-19.097	0
Cobicistat	-83.7343	-74.1677	-9.56651	0
Ruxolitinib	-82.5082	-71.6024	-10.9059	0
Fingolimod	-75.6867	-60.3308	-15.3559	0
Hydroxychloroquine	-74.8428	-66.1241	-8.71866	0
Chloroquine	-73.894	-65.431	-8.463	0
Arbidol	-69.6036	-63.6572	-5.9464	0

570

571

572 **Table 5** Interaction (hydrogen bonds and hydrophobic) of the top six compounds with
573 different amino-acids of the protease of SARS-COV-2

Ligand	H-Bond		Hydrophobic	
	Amino Acid	**Distance**	**Amino Acid**	**Distance**
60	SER 144	2.94	CYS 145	5.01; 5.49; 5.20; 5.04
	GLY 143	2.25	HIS 41	4.28
	CYS 145	2.46; 2.02	MET 165	5.37
			LEU 27	5.41
93	SER 144	2.87	GLN 189	2.78
	CYS 145	2.74	MET 165	4.92; 4.34
			CYS 145	5.49;
			LEU 27	4.13
34	HIS 164	2.47	MET 165	5.27
	SER 144	1.78	HIS 41	4.70
	GLY 143	1.84; 2.88	CYS 145	4.13
	ASN 142	3.02	LEU 27	4.88
	CYS 145	2.30		
55	GLU 166	2.90	HIS 41	4.88
	SER 144	2.33	LEU 27	4.75
	CYS 145	2.24; 2.45	CYS 145	4.30
42	CYS 145	2.51; 1.90	HIS 172	5.09
	HIS 164	3.12	HIS 163	5.48
	GLY 143	2.51	HIS 41	4.67
	SER 144	2.02	LEU 27	5.42
			CYS 145	4.98; 5.49; 5.22
58	CYS 145	2.22	MET 49	5.44
	SER 144	2.46	HIS 41	4.52; 4.63
	GLY 143	2.78	CYS 145	5.46
			MET 165	4.46
			HIS 163	3.72
			HIS 172	4.91
			PHE 140	5.01

574

575

576 **Table 6** LogS, LogD7.4 and LogP of the top six compounds

Property	**60**	**93**	**34**	**55**	**42**	**58**
Log S	-4.558	-4.664	-4.23	-4.581	-4.57	-4.558
$LogD_{7.4}$	2.754	2.728	0.958	2.702	2.765	2.754
LogP	3.908	4.274	3.723	3.908	4.018	3.908

577

578

579 **Table 7 Absorption properties of the top six thiazolidinones**

Property	**60**	**93**	**34**	**55**	**42**	**58**
Papp (Caco-2 Permeability)	-4.549	-4.566	-4.731	-4.528	-4.525	-4.549
Pgp-inhibitor	0.638	0.712	0.473	0.294	0.67	0.638
Pgp-substrate	0.036	0.09	0.033	0.042	0.086	0.036
HIA (Human Intestinal Absorption)	0.671	0.67	0.568	0.671	0.651	0.671
F (20% Bioavailability)	0.662	0.64	0.649	0.662	0.649	0.662
F (30% Bioavailability)	0.533	0.483	0.384	0.527	0.523	0.533

580

581

582 **Table 8 Distribution properties of top six thiazolidinones**

Property	**60**	**93**	**34**	**55**	**42**	**58**
PPB (%)	91.44	92.921	91.162	90.991	91.769	91.44
VD (L/kg)	-0.713	-0.892	-1.170	-0.702	-0.782	-0.713
BBB	0.615	0.679	0.269	0.788	0.647	0.615

583

584

585 **Table 9 Metabolism properties of top six thiazolidinones**

Property	**60**	**93**	**34**	**55**	**42**	**58**
P450 CYP1A2 inhibitor	0.591	0.615	0.608	0.68	0.678	0.591
P450 CYP1A2 Substrate	0.558	0.558	0.466	0.56	0.481	0.558
P450 CYP3A4 inhibitor	0.577	0.58	0.526	0.5	0.634	0.577
P450 CYP3A4 substrate	0.514	0.484	0.504	0.526	0.55	0.514
P450 CYP2C9 inhibitor	0.684	0.657	0.747	0.6	0.725	0.684
P450 CYP2C9 substrate	0.424	0.484	0.487	0.49	0.468	0.424
P450 CYP2C19 inhibitor	0.597	0.563	0.53	0.544	0.64	0.597
P450 CYP2C19 substrate	0.53	0.522	0.517	0.564	0.566	0.53
P450 CYP2D6 inhibitor	0.425	0.37	0.392	0.396	0.426	0.425
P450 CYP2D6 substrate	0.391	0.461	0.372	0.392	0.315	0.391

586

587

588 **Table 10 Excretion properties of top six thiazolidinones**

Property	**60**	**93**	**34**	**55**	**42**	**58**
$T_{1/2}$ (Half Life Time)	1.635	1.714	1.538	1.647	1.595	1.635
CL (Clearance Rate) mL/min/kg	1.075	1.104	1.007	1.022	0.943	1.075

589

590

591 **Table 11 Toxicity properties of top six thiazolidinones**

Property	**60**	**93**	**34**	**55**	**42**	**58**
hERG (hERG Blockers)	0.464	0.52	0.463	0.475	0.5	0.464
H-HT (Human Hepatotoxicity)	0.79	0.768	0.816	0.76	0.774	0.79
AMES (Ames Mutagenicity)	0.874	0.782	0.868	0.874	0.886	0.874
SkinSen (Skin sensitization)	0.561	0.476	0.546	0.561	0.545	0.561
LD50 (LD50 of acute toxicity)	2.831	3.604	3.052	2.863	3.072	2.831
DILI (Drug Induced Liver Injury)	0.898	0.902	0.89	0.898	0.884	0.898
FDAMDD (Maximum Recommended Daily Dose)	0.502	0.43	0.4	0.416	0.454	0.502

592

593